J-PARC BEAM COMMISSIONING PROGRESS

Hideaki Hotchi[#,1] and J-PARC beam commissioning team[1,2]
[1] Japan Atomic Energy Agency (JAEA), Tokai, Naka, Ibaraki, 319-1195 Japan
[2] High Energy Accelerator Research Organization (KEK), Tsukuba, Ibaraki, 305-0801 Japan

Abstract

The beam commissioning of the J-PARC began in November 2006 and it has well proceeded as planned so far. In this paper, the recent status of the J-PARC beam commissioning in the course of the beam power ramp-up scenario will be described especially focusing on the beam loss issues found in the current linac and RCS beam operation, and the results of beam tuning experiments recently performed in the RCS aiming at higher output beam power.

INTRODUCTION

The J-PARC is a multi-purpose proton accelerator facility aiming at MW-class output beam power. As shown in Fig. 1, the J-PARC accelerator complex comprises a chain of three accelerators (400-MeV H^- linac, a 3-GeV rapid cycling synchrotron; RCS, and a 50-GeV main ring synchrotron; MR) and three experimental facilities (a materials and life science experimental facility; MLF, a hadron experimental hall; HD, and a neutrino beam line to Kamioka; NU).

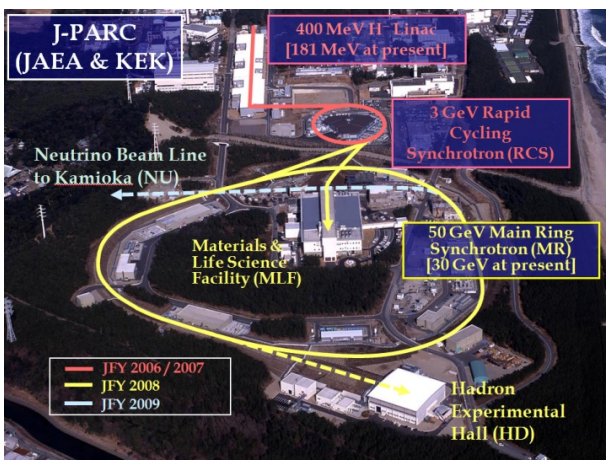

Figure 1: Bird's eye view of the J-PARC site.

The linac consists of an H^- ion source (IS), a radio frequency quadrupole (RFQ), a drift tube linac (DTL) and a separated-type DTL (SDTL). At full capability in the current configuration, the linac produces 36 kW output beam power at 181 MeV with a peak current of 30 mA, a pulse length of 0.5 ms, a chopper beam-on duty factor of 56% and a repetition rate of 25 Hz, which corresponds to 600 kW output at the RCS extraction energy of 3 GeV. The output energy of the linac will be upgraded to 400 MeV by adding an annular coupled structure (ACS) linac. The front-end system (IS and RFQ) will be also upgraded to get a peak current of 50 mA. Their installations are scheduled in 2013 summer-autumn period. The design output beam power of the upgraded linac is 133 kW, which corresponds to 1 MW output at the RCS extraction.

The H^- beam from the linac is delivered to the RCS injection point, where it is multi-turn charge-exchange injected with a carbon stripper foil. The RCS accelerates the injected protons up to 3 GeV with a repetition rate of 25 Hz. The current injection energy is 181 MeV. The RCS will first aim at 300–600 kW output with the lower injection energy, and then drive for the final goal of 1 MW output with the higher injection energy of 400 MeV after upgrading the linac in 2013.

The 3-GeV beam from the RCS is mainly transported to the MLF to produce pulsed spallation neutrons and muons. A part of the RCS beam (typically four pulses every several seconds) is transported to the MR. The MR still accelerates the injected beam to 30 GeV (it will be upgraded to 50 GeV in the second phase of the J-PARC project), delivering it to the HD by slow extraction and to the NU by fast extraction. The design output beam power of the MR is 750 kW.

The beam commissioning of the J-PARC began in November 2006 from the linac to the downstream facilities. Via a series of initial beam tuning tests [1], we started the user program for the MLF in December 2008, for the HD in February 2009, and for the NU in January 2010. The output beam power has been gradually increased following the progression of beam tuning and hardware improvements, with carefully monitoring the trend of machine activation levels. The current output beam power from the RCS to the MLF is 220 kW, and the MR delivers 145 kW beam to the NU by fast extraction and 3.6 kW beam to the HD by slow extraction.

In this paper, the current status of the J-PARC beam commissioning in the course of the beam power ramp-up scenario will be described especially focusing on the beam loss issues found in the current linac and RCS beam operation, and the results of beam tuning experiments recently performed in the RCS aiming at higher output beam power. The recent progress of the MR beam commissioning is described in more detail in Ref. [2].

BEAM LOSS ISSUES FOUND IN THE CURRENT LINAC AND RCS BEAM OPERATION

The linac and RCS have performed 220 kW routine user operations to the MLF since November 2010. In this section, we summarize beam loss issues found in the current linac and RCS beam operation.

#hotchi.hideaki@jaea.go.jp

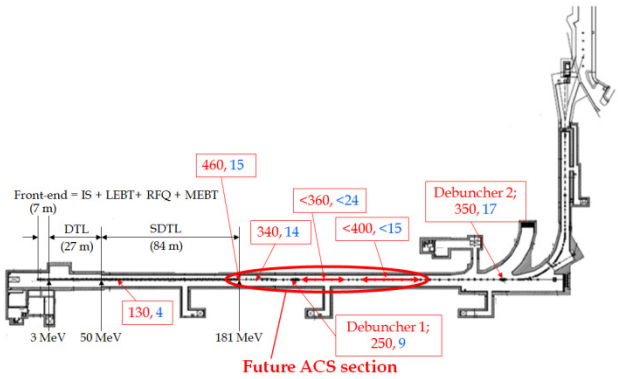

Figure 2: Residual radiation level (μSv/h) in the linac measured 4-hour after the shutdown of 220-kW beam operation to the MLF, where the red one is for the measurement on the surface of the vacuum chamber, and the blue one is for the measurement at a distance of 30 cm.

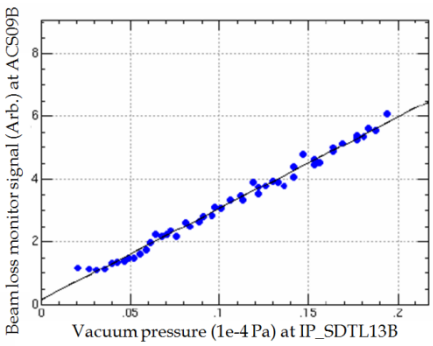

Figure 3: Vacuum pressure dependence of the beam loss monitor signal at the future ACS section.

Linac

Figure 2 shows a typical residual radiation level in the linac measured 4-hour after the shutdown of 220-kW beam operation to the MLF, where the red one is for the measurement on the surface of the vacuum chamber, and the blue one is for the measurement at a distance of 30 cm. While the machine activation in the linac is sufficiently low in the current 220-kW beam operation, the residual activations (several hundreds μSv/h on the chamber surface) widely distributed over the future ACS section has to be solved for realizing higher beam power operations. As shown in Fig. 3, the beam loss at the future ACS section has a linear response for the vacuum pressure, and the extrapolated line practically has no intercept [3]. These results indicate that the main cause of this particle loss is H^0 component arising from residual gas stripping. In order to get further beam loss reduction, it is necessary to make a further improvement of the vacuum system in this area.

RCS

Figure 4 shows a typical residual radiation level in the RCS measured 4-hour after the shutdown of 220-kW beam operation to the MLF. The current beam loss in the RCS is sufficiently small, most of which is well localized in the ring collimator section. But we have some beam loss issues to be solved for aiming at higher power operations.

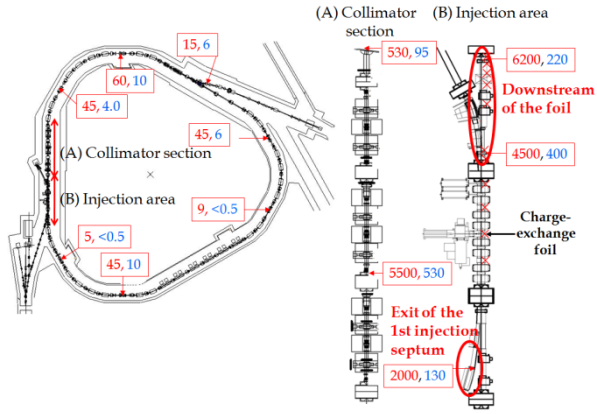

Figure 4: Residual radiation level (μSv/h) in the RCS measured 4-hour after the shutdown of 220-kW beam operation to the MLF, where the red one is for the measurement on the surface of the vacuum chamber, and the blue one is for the measurement at a distance of 30 cm.

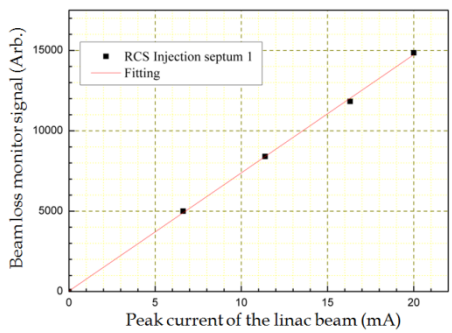

Figure 5: Beam loss monitor signal at the exit of 1st injection septum measured as a function of the peak current of the injection beam.

First is the machine activation (2000 μSv/h on the chamber surface) at the exit of the 1st injection septum in the injection beam line. This residual dose is observed only at the outer side of the beam line, at which the beam loss monitor signal has no significant response for orbit changes. Also the beam loss monitor signal has a linear response for the peak current of the injection beam [4], as shown in Fig. 5. These results imply that the main cause of this beam loss is H^0 component arising from residual gas stripping. For this concern, we will investigate the vacuum pressure dependence of the beam loss, and if it shows a positive sign of beam loss reduction, we will improve the vacuum system in the injection beam line.

Another issue is the machine activation (5000–6000 μSv/h on the chamber surface) downstream of the charge-exchange foil, which arises from the foil scattering beam loss. In the RCS, a multi-turn charge-exchange injection with a carbon foil is adopted. In this way, the beam hits the foil many times during injection period. As shown in

Fig. 6, the beam loss monitor signals located at the hot spots are proportional to the foil hitting rate during injection. This is clear evidence that the machine activations come from the foil scattering. Figure 7 shows a result of the tracking simulation for scattered particles on the foil [5], where the particles are generated at the foil position using the scattering angle distribution calculated with GEANT. This tracking simulation well reproduces the observed beam loss points and shows that large angle events with a scattering angle of 20–25 mrad make the observed machine activations. In order to localize the foil scattering beam loss, we will introduce a new collimation system [5], as shown in the lower plot of Fig. 7. The construction of the collimator is in progress now, and it will be installed in the present beam shutdown period.

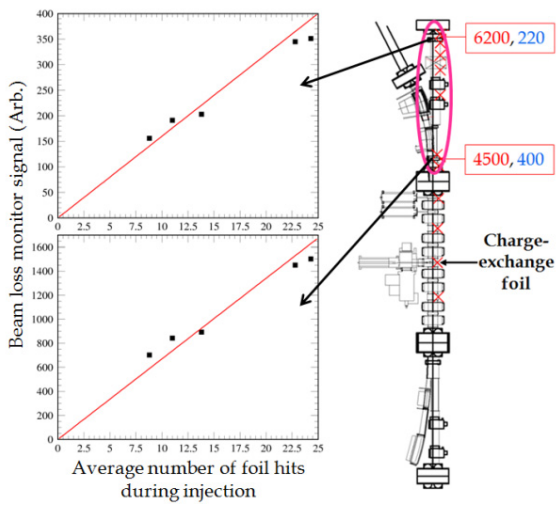

Figure 6: Beam loss monitor signals at the hot spots downstream of the charge-exchange foil measured as a function of the foil hitting rate during injection.

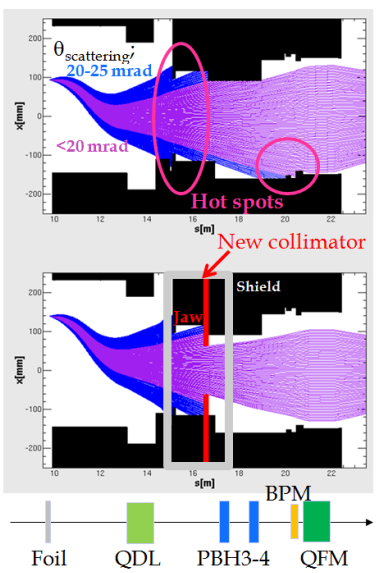

Figure 7: Tracking simulation for scattered particles on the charge-exchange foil.

BEAM STUDY RESULTS OF THE RCS

The recent progress of the RCS beam study is described in this section.

Beam-Based Measurements of Lattice Imperfections

In the RCS, the beam injection is performed with a local bump orbit formed by four sets of horizontal pulse dipole magnets, in which the issue is that the edge focus at the entrance and exit of the injection bump magnets modulates the betatron amplitude function. This beta modulation makes a distortion of the lattice super-periodicity, driving random lattice resonances. Figure 8 shows the result of beta modulation measurement. In the present four-bump method, the beta modulation is caused especially in the vertical plane. From this measurement, the strength of the edge focus was evaluated to be –0.0033 m^{-1}, which corresponds to around 1% of the main quadrupole field strength.

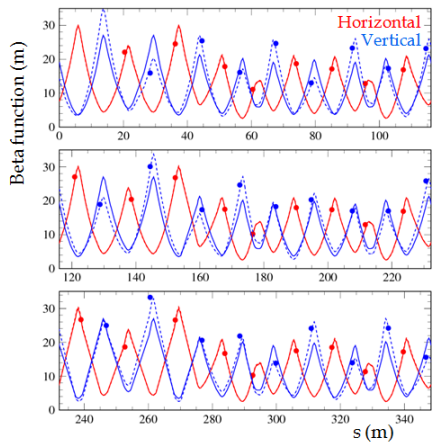

Figure 8: Beta modulation caused by the edge focus of the injection bump magnets, where the circles correspond to the measured ones when the injection bump is on, and the solid curves show the design beta function when the injection bump is off.

In addition, we have a local field error in the extraction section, which arises from a field leakage from the extraction beam line DC magnets. Figure 9 shows a COD caused by the leakage field. From this COD data, the dipole field component of the leakage field was evaluated to be 1.14 (horizontal) and 0.12 (vertical) mrad. In addition to the dipole field component, we found that the leakage field includes normal and skew quadrupole field components and affects the beam through a distortion of the lattice super-periodicity and linear coupling. The normal quadrupole component in the leakage field was estimated to be 0.0048 m^{-1} from the optics measurements. On the other hand, the skew quadrupole component in the leakage field was estimated to be –0.00112 m^{-1} from horizontal-vertical coupling measurements, namely by observing an orbit leak to the vertical plane by a horizontal single kick (Fig. 10-A), and also by systematic measurement of two normal mode tunes near a linear

coupling resonance (Fig. 10-B).

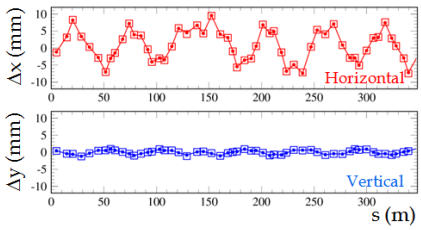

Figure 9: COD caused by the leakage field from the extraction beam line magnets, where the circles are the measured ones, and the squares are the calculated ones.

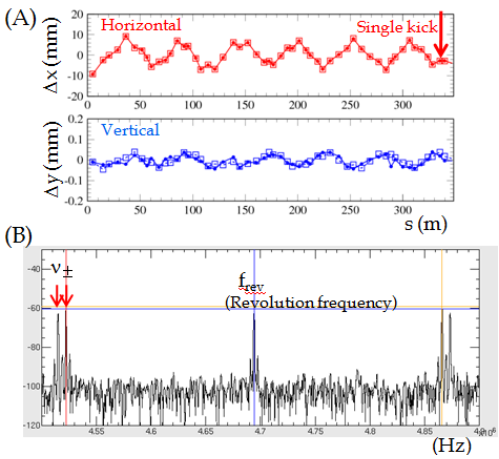

Figure 10: (A) Orbit leak to the vertical plane by a horizontal single kick, where the circles are the measured ones and the squares are the calculated ones. (B) FFT spectrum of the beam position monitor signal, where the two arrows correspond to two normal mode betatron tunes observed near a linear coupling resonance.

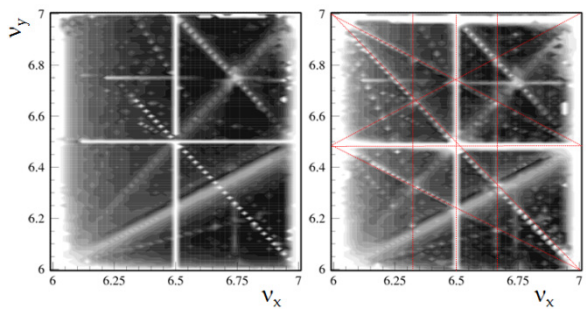

Figure 11: Tune diagrams calculated without (left) and with (right) the edge focus of the injection bump magnets and the leakage field from the extraction beam line magnets.

Figure 11 shows tune diagrams calculated without and with the edge focus and the leakage field. In the figure, we can see that the linear coupling resonance and the 3rd-order random resonances are enhanced by the edge focus and the leakage field, and they make a strong limit for the tune-ability. In order to get more stable and flexible tune space, we plan to install additional magnetic shields for reducing the leakage field, and introduce quadrupole correctors for compensating the edge focus effect. These hardware improvements are scheduled in 2012 and 2013 summer maintenance periods.

Our understanding of the basic lattice property was deepened through such a series of beam dynamics measurements.

High Intensity Trial – Beam Loss Reduction by Painting Injection

We have recently performed a high intensity trial using a 0.5 ms-long linac pulse with a peak current of 20 mA and a chopper beam-on duty factor of 56%. In this case, the number of particles per pulse totals 3.5×10^{13}, corresponding to 420 kW output beam power at a repetition rate of 25 Hz. For this injection beam, we tried to reduce the beam loss arising from the space charge effect in the low energy region employing the transverse [6] and longitudinal [7, 8] painting injection techniques, where the operating tune was chosen at (6.45, 6.42) to avoid a possible effect of strong betatron resonances.

Table 1: Painting Injection Parameters

Data ID	ε_{tp} (π mm mrad)	V_2/V_1 (%)	ϕ_2 (degrees)	Δp/p (%)
1	-	-	-	-
2	-	80	−100	-
3	-	80	−100	−0.1
4	-	80	−100	−0.2
5	50	80	−100	−0.2
6	100	80	−100	−0.2

Table 1 shows the parameters of transverse and longitudinal painting applied in this beam study. In the transverse plane, correlated painting with a painting emittance of 50π and 100π mm mrad (ε_{tp}) was mainly applied. On the other hand, longitudinal painting was performed by the momentum offset injection of 0 to −0.2% (Δp/p) in combination with superposing a second harmonic rf with an amplitude of 80% of the fundamental (V_2/V_1). The phase sweep from −100 to 0 degrees of the second harmonic rf relative to the fundamental (ϕ_2) was also employed, which enables to control the bunch distribution through a dynamic change of the rf bucket potential. With systematic combination of transverse and longitudinal painting parameters listed in Table 1, we investigated their effectiveness for beam loss reduction.

Figure 12 shows the measured beam survival rate in the RCS (ratio of the output and input intensities), where the horizontal axis is the painting parameter ID number listed in Table 1. As shown by data ID 1, the beam survival rate in the case of no painting was measured to be 83%. In order to reduce the observed 17% intensity loss, we introduced the painting injection. As shown in Fig. 12, the beam survival was gradually improved from data ID 1 to 4 by introducing longitudinal painting, from data ID 4 to

6 by adding transverse painting.

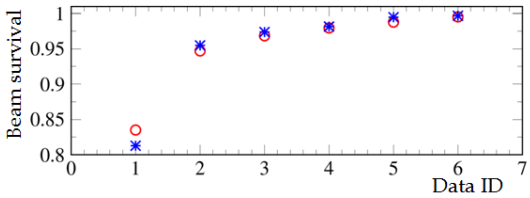

Figure 12: Measured beam survival rate (red circles), where the horizontal axis corresponds to the painting parameter ID number in Table 1. The blue stars are the corresponding numerical simulation results.

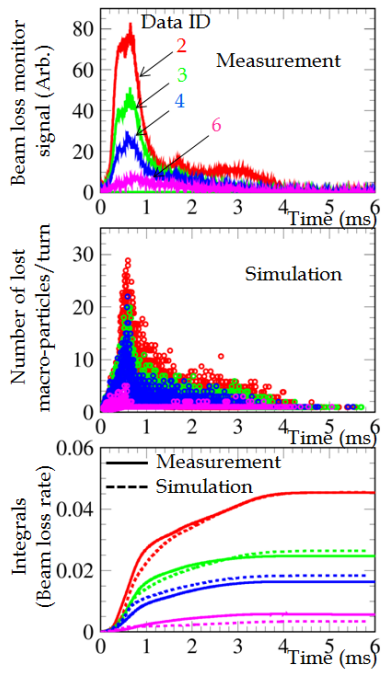

Figure 13: (Top) Scintillation type beam loss monitor signal for the first 6 ms measured in the collimator section for data ID 2 to 6 in Table 1. (Middle) Corresponding numerical simulation results plotted as a number of lost macro particles per turn. (Bottom) Integrated curves of measured and simulated beam loss distribution in the top and middle plots, where the simulated curves are normalized to be the beam loss rate, and the measured curves are scaled to fit the simulated patterns.

The top plot in Fig. 13 shows the scintillation-type beam loss monitor signal for the first 6 ms measured in the collimator section for data ID 2 to 6. In the figure, we can clearly see the time structure of the beam loss; the beam loss appears only for the first 4 ms where the space charge effect is most severe, which is effectively reduced with the progression of the painting injection.

The best beam survival rate obtained for the parameter ID 6 was better than 99%, where the highest output intensity, corresponding to 420 kW output beam power, was obtained. This achievement of the low-loss beam operation is considered to be a large step toward realizing our final goal of 1 MW output, because the present 420 kW beam operation gives more severe space-charge effect at the lower injection energy of 181 MeV than that at the higher injection energy of 400 MeV in the 1 MW beam operation as per the $\beta^2\gamma^3$ scaling law.

High Intensity Trial – Beam Loading Compensation

High intensity accelerations involve an rf bucket distortion arising from multi-harmonic components of the beam loading, and its compensation is a key issue to realize higher power operation. Such a beam loading effect is now well compensated by the multi-harmonic rf feed-forward method [9]. Therefore the beam is now well accelerated with feeling the accelerating voltage as programmed. The beam loss arising from the distortion of the rf bucket is now negligible thanks to the beam loading compensation.

SUMMARY AND FUTURE PLAN

The J-PARC accelerators have started the user program for the MLF, NU and HD. The output beam power has been steadily increased following the progression of beam tuning and hardware improvements. The current RCS output beam power to the MLF is 220 kW, and the MR delivers 145 kW beam to the NU by fast extraction and 3.6 kW beam to the HD by slow extraction.

The RCS has recently performed a high intensity trial with 420 kW-equivalent intensity beam, in which we got several significant progresses leading to realizing the design output beam power of 1 MW, such as beam loss reduction by the painting injection technique, and beam loading compensation by the multi-harmonic rf feed-forward method.

Now the J-PARC is in the shutdown period to recover the damages caused by the East Japan earthquake on March 11, 2011 [10]. The recovery work is in progress almost as planned. The J-PARC will restart the beam test in December 2011, and then the user operation in January 2012. The next goal of the J-PARC beam commissioning is to realize the output beam power of 300 kW from the RCS and 200–300 kW from the MR (fast extraction mode) before upgrading the linac. The installations of the ACS for 400 MeV acceleration and the new RFQ and IS to get a peak current of 50 mA are scheduled in 2013 summer-autumn period. The beam commissioning of the upgraded linac will start by the end of 2013.

REFERENCES

[1] H. Hotchi et al., PRST-AB 12, 040402 (2009).
[2] T. Koseki, in these proceedings, WEPS008.
[3] G. Wei, in these proceedings, WEPS048.
[4] K. Yamamoto, Proc. of HB2010, TUO2C06.
[5] K. Yamamoto et al., in these proceedings, TUPS033.
[6] P.K. Saha et al., PRST-AB 12, 040403 (2009).
[7] F. Tamura et al., PRST-AB 12, 041001 (2009).
[8] M. Yamamoto et al., NIM, A 621, 15 (2010).
[9] F. Tamura et al., PRST-AB 14, 051004 (2011).
[10] K. Hasegawa et al., in these proceedings, WEPS095.